

Supporting information

Dimeric complexes of rare-earth substituted Keggin-type silicotungstates: Syntheses, crystal structure and solid state properties

Mukesh Kumar Saini,^a Rakesh Gupta,^a Swati Parbhakar,^a Anil Kumar Mishra,^b Rashi Mathur,^b and Firasat Hussain^{*a}

Table of Contents-

Fig. S1 FT-IR spectra of $\text{Na}_4\text{K}_8[\{\text{Ln}(\alpha\text{-SiW}_{11}\text{O}_{39})(\text{H}_2\text{O})\}_2(\mu\text{-CH}_3\text{COO})_2] \cdot x\text{H}_2\text{O}$ [Ln = Eu^{III} (**Eu-1a**), Gd^{III} (**Gd-2a**), Tb^{III} (**Tb-3a**), Dy^{III} (**Dy-4a**), Ho^{III} (**Ho-5a**), Er^{III} (**Er-6a**), and Tm^{III} (**Tm-7a**)] (recorded on KBr pellets).

Fig. S2 FT-IR spectra of $\text{Na}_4\text{K}_8[\{\text{Tm}(\alpha\text{-SiW}_{11}\text{O}_{39})(\text{H}_2\text{O})\}_2(\mu\text{-CH}_3\text{COO})_2] \cdot 26\text{H}_2\text{O}$ (**Tm-7a**) POM, $\text{Na}_{10}[\alpha\text{-SiW}_9\text{O}_{34}] \cdot 16\text{H}_2\text{O}$ and $\text{K}_8[\alpha\text{-SiW}_{11}\text{O}_{39}] \cdot 13\text{H}_2\text{O}$ (recorded on KBr pellets).

Fig. S3 FT-IR spectra of $\text{K}_6\text{Na}_7[\text{Ln}(\text{SiW}_{11}\text{O}_{39})_2] \cdot x\text{H}_2\text{O}$ [Ln = Pr^{III} (**Pr-8a**), Nd^{III} (**Nd-9a**), and Sm^{III} (**Sm-10a**)] POMs (recorded on KBr pellets).

Fig. S4 Solid state UV/vis spectrum of $\text{Na}_4\text{K}_8[\{\text{Dy}(\alpha\text{-SiW}_{11}\text{O}_{39})(\text{H}_2\text{O})\}_2(\mu\text{-CH}_3\text{COO})_2] \cdot 30\text{H}_2\text{O}$ (**Dy-4a**).

Fig. S5 Photoluminescence spectrum of $\text{Na}_4\text{K}_8[\{\text{Tb}(\alpha\text{-SiW}_{11}\text{O}_{39})(\text{H}_2\text{O})\}_2(\mu\text{-CH}_3\text{COO})_2] \cdot 22\text{H}_2\text{O}$ (**Tb-3a**).

Fig. S6 Thermogravimetric analysis data of $\text{Na}_4\text{K}_8[\{\text{Ln}(\alpha\text{-SiW}_{11}\text{O}_{39})(\text{H}_2\text{O})\}_2(\mu\text{-CH}_3\text{COO})_2] \cdot x\text{H}_2\text{O}$ [Ln = Eu^{III} (**Eu-1a**), Gd^{III} (**Gd-2a**), Tb^{III} (**Tb-3a**), Dy^{III} (**Dy-4a**), Ho^{III} (**Ho-5a**), Er^{III} (**Er-6a**), and Tm^{III} (**Tm-7a**)].

Fig. S7 Thermogravimetric analysis data of $\text{K}_6\text{Na}_7[\text{Ln}(\text{SiW}_{11}\text{O}_{39})_2] \cdot x\text{H}_2\text{O}$ [Ln = Pr^{III} (**Pr-8a**), Nd^{III} (**Nd-9a**), and Sm^{III} (**Sm-10a**)].

Fig. S8 UV/vis spectra of $\text{Na}_4\text{K}_8[\{\text{Ln}(\alpha\text{-SiW}_{11}\text{O}_{39})(\text{H}_2\text{O})\}_2(\mu\text{-CH}_3\text{COO})_2] \cdot x\text{H}_2\text{O}$ [Ln = Eu^{III} (**Eu-1a**), Gd^{III} (**Gd-2a**), Tb^{III} (**Tb-3a**), Dy^{III} (**Dy-4a**), Ho^{III} (**Ho-5a**), Er^{III} (**Er-6a**), and Tm^{III} (**Tm-7a**)].

Fig. S9 ¹H NMR data of **Eu-1a**, **Gd-2a**, **Tb-3a**, **Dy-4a**, **Eu-5a**, **Er-6a** and **Tm-7a** POMs.

Fig. S10 ¹³C NMR data of **Eu-1a**, **Gd-2a**, **Tb-3a**, **Dy-4a**, **Eu-5a**, **Er-6a** and **Tm-7a** POMs.

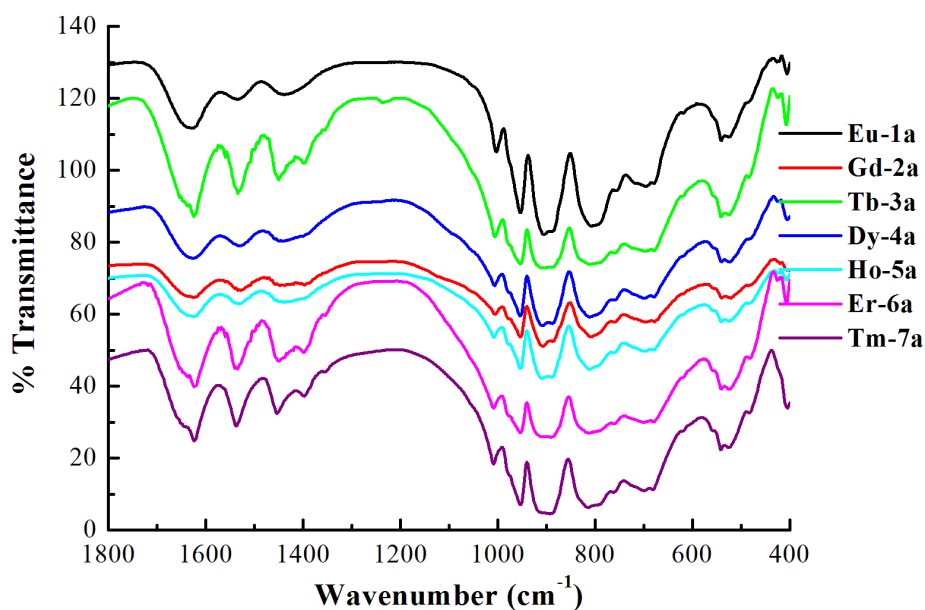


Fig. S1 FT-IR spectra of $\text{Na}_4\text{K}_8\{[\text{Ln}(\alpha\text{-SiW}_{11}\text{O}_{39})(\text{H}_2\text{O})_2](\mu\text{-CH}_3\text{COO})_2\} \cdot x\text{H}_2\text{O}$ [Ln = Eu^{III} (**Eu-1a**), Gd^{III} (**Gd-2a**), Tb^{III} (**Tb-3a**), Dy^{III} (**Dy-4a**), Ho^{III} (**Ho-5a**), Er^{III} (**Er-6a**), and Tm^{III} (**Tm-7a**)] (recorded on KBr pellets).

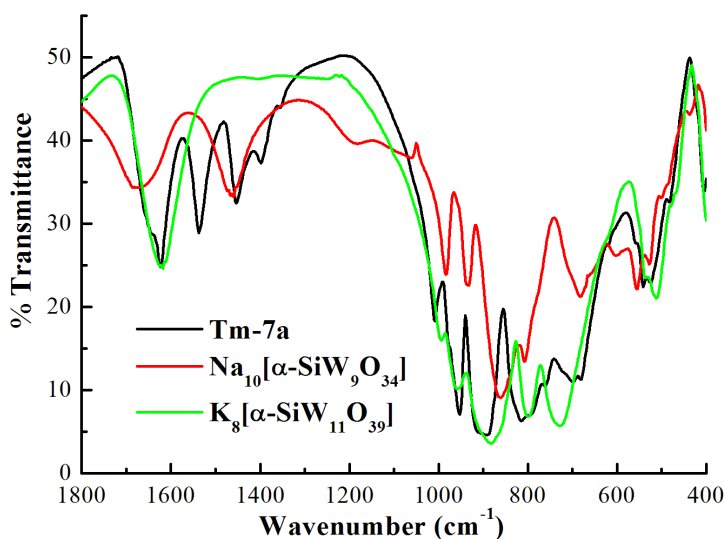


Fig. S2 FT-IR spectra of **Tm-7a** POM, $\text{Na}_{10}[\alpha\text{-SiW}_9\text{O}_{34}] \cdot 16\text{H}_2\text{O}$ and $\text{K}_8[\alpha\text{-SiW}_{11}\text{O}_{39}] \cdot 13\text{H}_2\text{O}$ (recorded on KBr pellets)

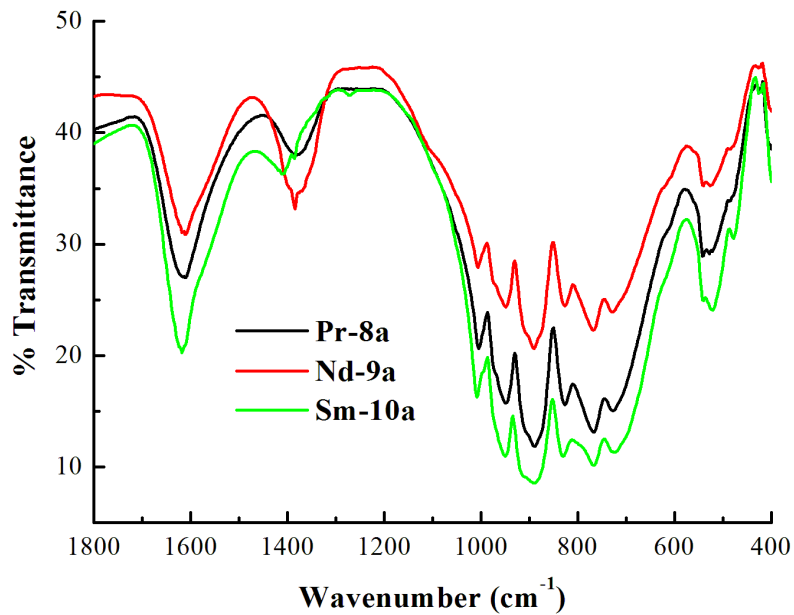


Fig. S3 FT-IR spectra of $\text{K}_6\text{Na}_7[\text{Ln}(\text{SiW}_{11}\text{O}_{39})_2] \cdot x\text{H}_2\text{O}$ [$\text{Ln} = \text{Pr}^{\text{III}}$ (**Pr-8a**), Nd^{III} (**Nd-9a**), and Sm^{III} (**Sm-10a**)] POMs (recorded on KBr pellets).

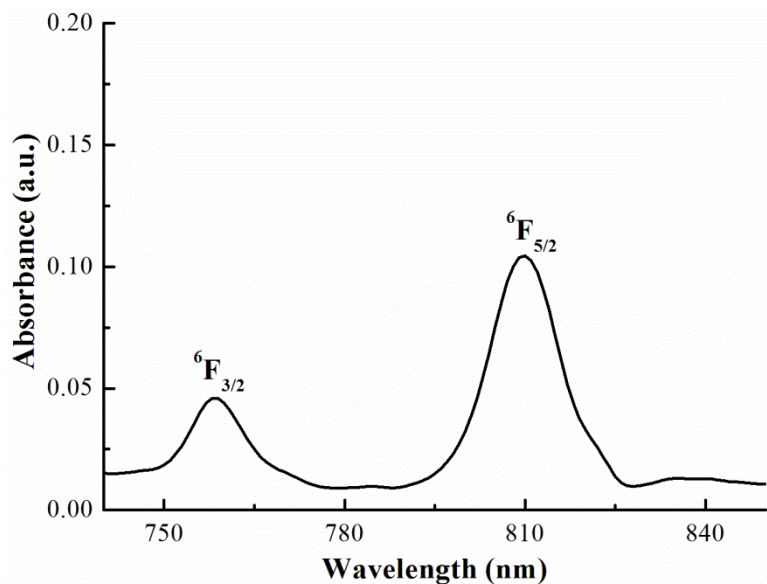


Fig. S4 Solid state UV/vis spectrum of $\text{Na}_4\text{K}_8[\{\text{Dy}(\alpha\text{-SiW}_{11}\text{O}_{39})(\text{H}_2\text{O})\}_2(\mu\text{-CH}_3\text{COO})_2] \cdot 30\text{H}_2\text{O}$ (**Dy-4a**).

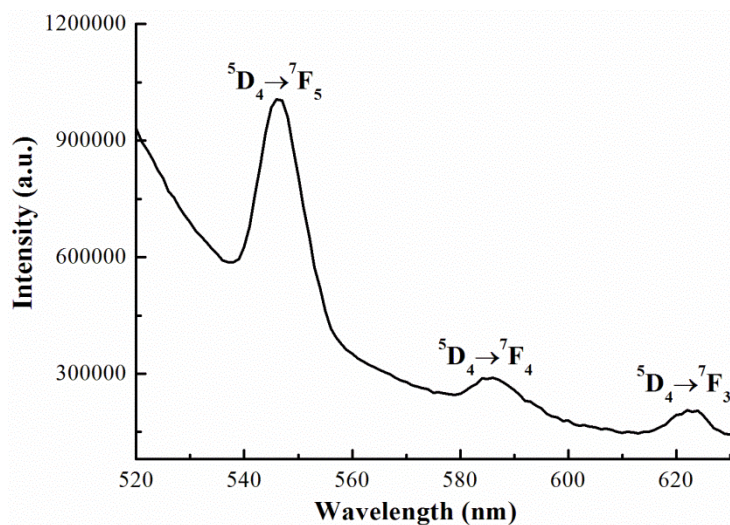


Fig. S5 Photoluminescence spectrum of $\text{Na}_4\text{K}_8\{[\text{Tb}(\alpha\text{-SiW}_{11}\text{O}_{39})(\text{H}_2\text{O})]_2(\mu\text{-CH}_3\text{COO})_2\} \cdot 22\text{H}_2\text{O}$ (**Tb-3a**).

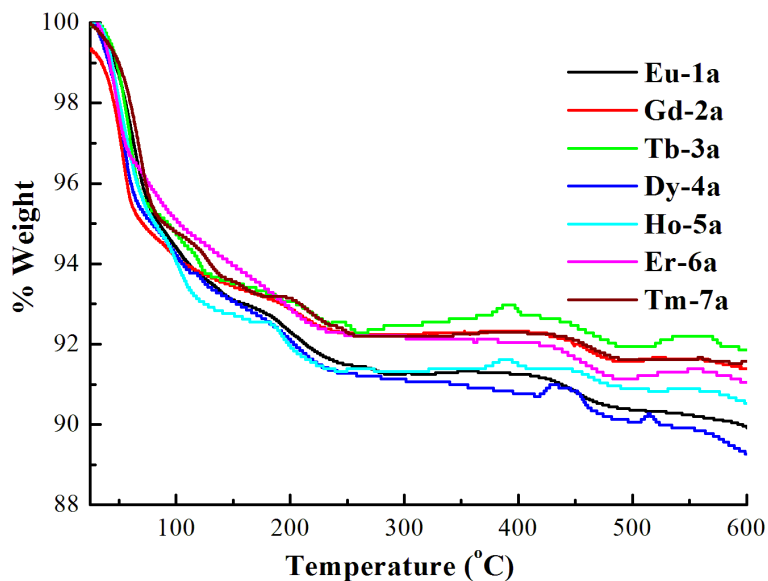


Fig. S6 Thermogravimetric analysis data of $\text{Na}_4\text{K}_8\{[\text{Ln}(\alpha\text{-SiW}_{11}\text{O}_{39})(\text{H}_2\text{O})]_2(\mu\text{-CH}_3\text{COO})_2\} \cdot x\text{H}_2\text{O}$ [$\text{Ln} = \text{Eu}^{\text{III}}$ (**Eu-1a**), Gd^{III} (**Gd-2a**), Tb^{III} (**Tb-3a**), Dy^{III} (**Dy-4a**), Ho^{III} (**Ho-5a**), Er^{III} (**Er-6a**), and Tm^{III} (**Tm-7a**)].

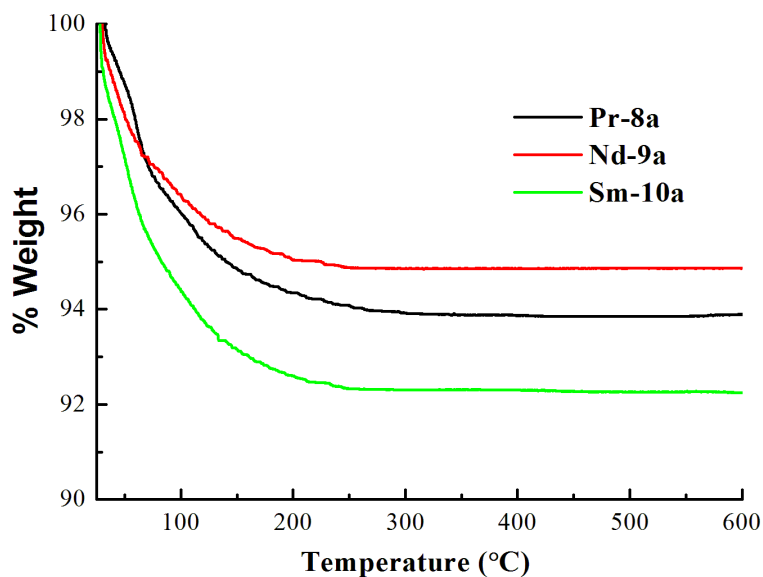


Fig. S7 Thermogravimetric analysis data of $\text{K}_6\text{Na}_7[\text{Ln}(\text{SiW}_{11}\text{O}_{39})_2] \cdot x\text{H}_2\text{O}$ [$\text{Ln} = \text{Pr}^{\text{III}}$ (**Pr-8a**), Nd^{III} (**Nd-9a**), and Sm^{III} (**Sm-10a**)].

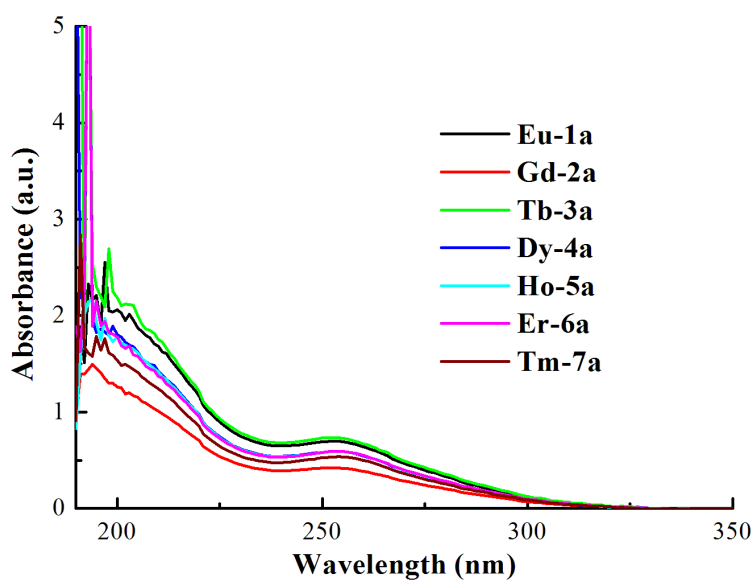


Fig. S8 UV/vis spectra of $\text{Na}_4\text{K}_8[\{\text{Ln}(\alpha\text{-SiW}_{11}\text{O}_{39})(\text{H}_2\text{O})\}_2(\mu\text{-CH}_3\text{COO})_2] \cdot x\text{H}_2\text{O}$ [$\text{Ln} = \text{Eu}^{\text{III}}$ (**Eu-1a**), Gd^{III} (**Gd-2a**), Tb^{III} (**Tb-3a**), Dy^{III} (**Dy-4a**), Ho^{III} (**Ho-5a**), Er^{III} (**Er-6a**), and Tm^{III} (**Tm-7a**)].

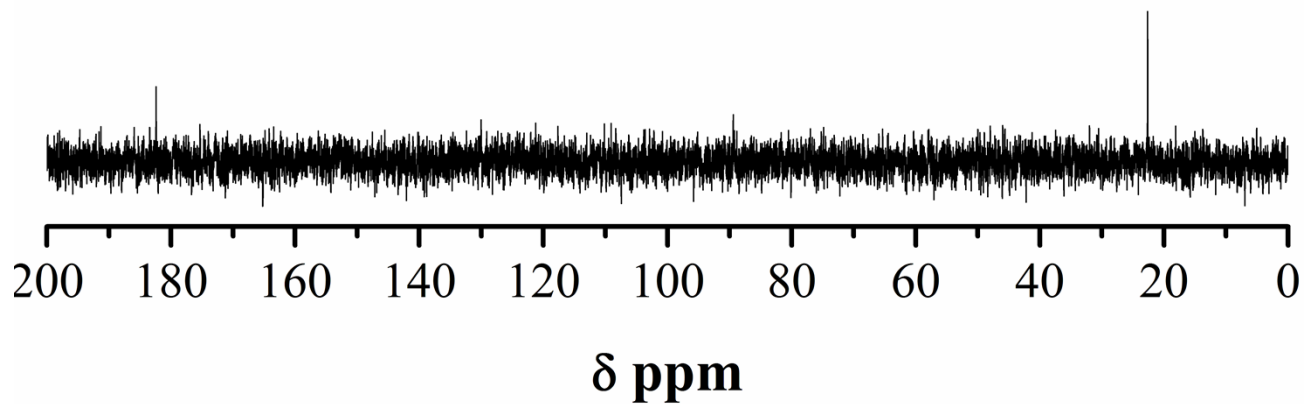


Fig. S9 ^{13}C NMR data of **Eu-1a**, POMs

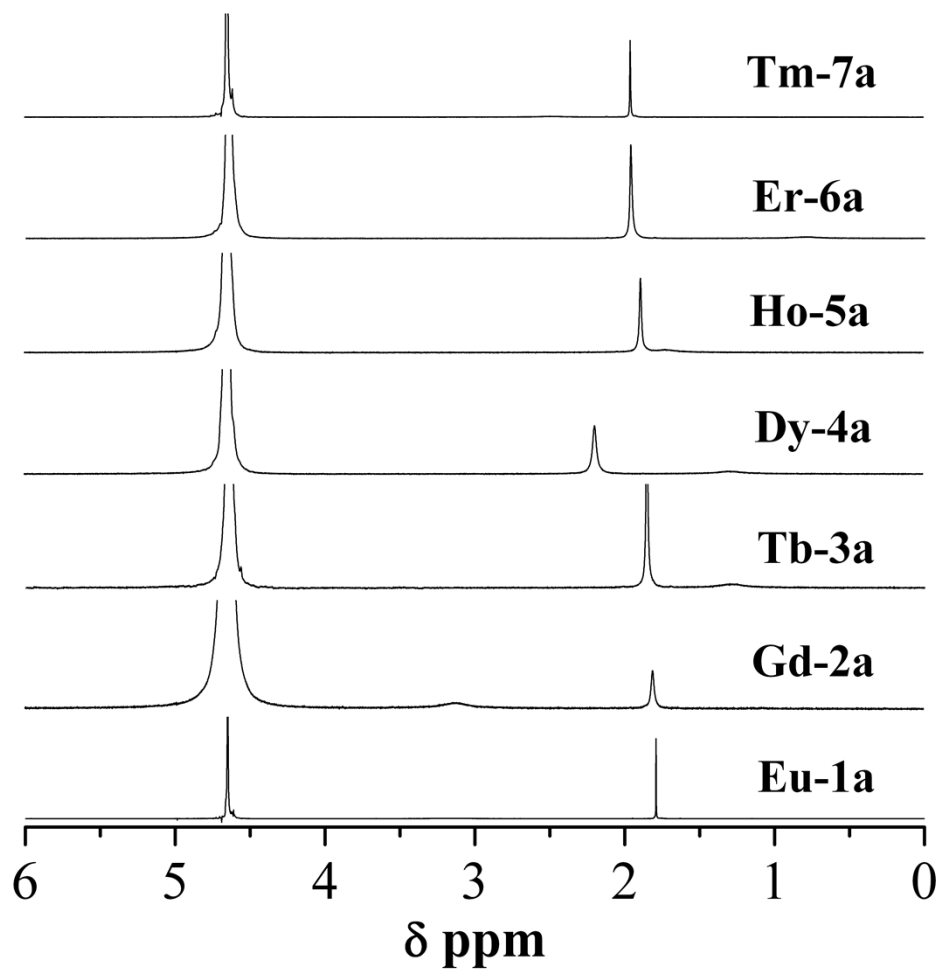


Fig. S10 ^1H NMR data of **Eu-1a**, **Gd-2a**, **Tb-3a**, **Dy-4a**, **Eu-5a**, **Er-6a** and **Tm-7a** POM